Current Science
CS 5 (3), 2998-3010 (2025)
Received 24 March 2025 | **Revised 18 April** 2025 | **Accepted 22 May**. 2025 | **Online Available 14 June** 2025
https://doi.org/ 10.52845/CS/2025-5-3-70

Current Science
Current Science

OPEN ACCESS **ISSN(O)2795-8639**

Original Article

Rock Mass Point Cloud Registration Based on Feature Extraction and Polyhedral Topology Mapping

Wugen Liu[1], Weichao Lu[2], Yijing Li[3]*, Yuekang Li[4], Wang Zhou[5]

[1]Shangrao Guokong Engineering Testing Co., Ltd, 330031, China

[2]School of Civil Engineering and Architecture, Nanchang University, Nanchang 330031, China

[3]School of Civil Engineering and Architecture, Nanchang University, Nanchang 330031, China

[4]School of Civil Engineering and Architecture, Nanchang University, Nanchang 330031, China

[5]School of Civil Engineering and Architecture, Nanchang University, Nanchang 330031, China

[*]Corresponding Author: Yijing Li

Abstract:
Rock mass point cloud registration is a fundamental step in studying the three-dimensional characteristics of rock masses. The complex geometry and uneven density distribution of rock surfaces often complicate feature extraction, affecting registration accuracy. Addressing these issues, we propose a novel registration algorithm that utilizes neighborhood multi-dimensional feature extraction and spatial tetrahedral descriptors. We integrate point cloud density, normal vectors, and surface curvature to extract clusters of feature points, and take the centroid of these clusters as the feature points of the rock mass. Then, we construct spatial tetrahedron descriptors for the feature points to identify corresponding points and calculate transformation matrices for coarse registration. Subsequently, the Iterative Closest Point (ICP) algorithm is applied for fine registration. The experiments conducted on the Rock bench dataset, WHU-TLS dataset, and real-world dataset show that the proposed method extracts more comprehensive and accurate feature points than curvature based feature algorithms, normal based feature extraction algorithms, Gaussian curvature algorithms, and SVF algorithms. Applying the feature points extracted by each method to the spatial tetrahedral descriptor proposed in this paper for coarse registration, and then using the ICP algorithm for fine registration, our accuracy improved by 96.06%, 94.3%, 65.6%, and 77.8% compared to other methods.
Finally, this article analyzed the overlap and initial position robustness of the registration method, and compared its accuracy with ICP, LM-ICP, and NDT methods, demonstrating the effectiveness of this method.
Keywords: feature extraction, point cloud, registration, rock mass, descriptor.

1. Introduction

The study of three-dimensional characteristics of rock masses provides strong data support and decision-making tools for fields such as geological engineering, resource exploration, environmental monitoring, landslide prevention and control (Huang et al., 2024), and cultural heritage protection.

Many studies use the structural lines, surfaces, and feature points on the surface of rock masses as corresponding elements to achieve registration. Liu et al. (2022) first used hyper voxel segmentation technology to extract the surface of rock masses, then extracted feature lines from the boundaries of the extracted rock mass surface, and finally selected feature points for registration from these feature lines. Hu et al. (2020) used an effective region growing algorithm to detect planes from rock point clouds, and then calculated the corresponding polygon boundary features using the concave shell method. However, using line and plane features for registration is only suitable for sedimentary rocks with obvious surface bedding structures, and is not suitable for igneous rocks with rounded surfaces.

Wang et al. (2019) extracted rock feature points through point cloud surface curvature and constructed a complete map of n points to find the corresponding relationships between feature points for registration. Wang et al. (2021) defined SVF values by constructing sum vectors between neighboring points, and used SVF values to screen rock surface feature points. However, when using 3D laser scanning technology to collect large rock point clouds, the uneven distribution of point cloud density due to distance and scanning angle affects the accuracy of feature point extraction and registration.

Constructing stable descriptors for extracted feature elements and matching corresponding elements is an important step in unifying the coordinates of two point clouds. Methods such as 3D Shape Context （3DSC） （Frome et al., 2004） , fast point feature histogram（FPFH） （ Rusu et al., 2009）, Direction Histogram Signature（SHOT） （Tombari et al., 2010） , and Radius based Surface Descriptors（RSD） （ Warchol, 2018） all find the correspondence between two sets of point clouds by describing the local neighborhood information of feature points.

However, the surface of the rock mass lacks effective contextual information, the texture structure is irregular, and the roughness distribution is anisotropic. The local neighborhood information of feature points cannot stably capture corresponding relationships.

In response to the above issues, we integrate the point cloud distribution density, normal direction, and surface curvature to jointly describe the surface features of the rock mass, and use clustering algorithms to extract feature points for registration. In order to accurately obtain the correspondence between two sets of rock point clouds, we constructed a spatial tetrahedral descriptor, used the neighborhood relationship of each feature point on the entire rock mass to achieve corresponding point pairing, and calculated the coordinate transformation matrix.

2. Methodology

The method includes the following steps: First, integrate point cloud normal, surface curvature, and point cloud density to extract feature points of the rock mass; Then, cluster feature points to obtain the centroid; Subsequently, construct spatial tetrahedrons to find corresponding points between the source and target point clouds; Finally, calculate the transformation matrix. For a better understanding, we will place the overall framework and each step in Figure 1.

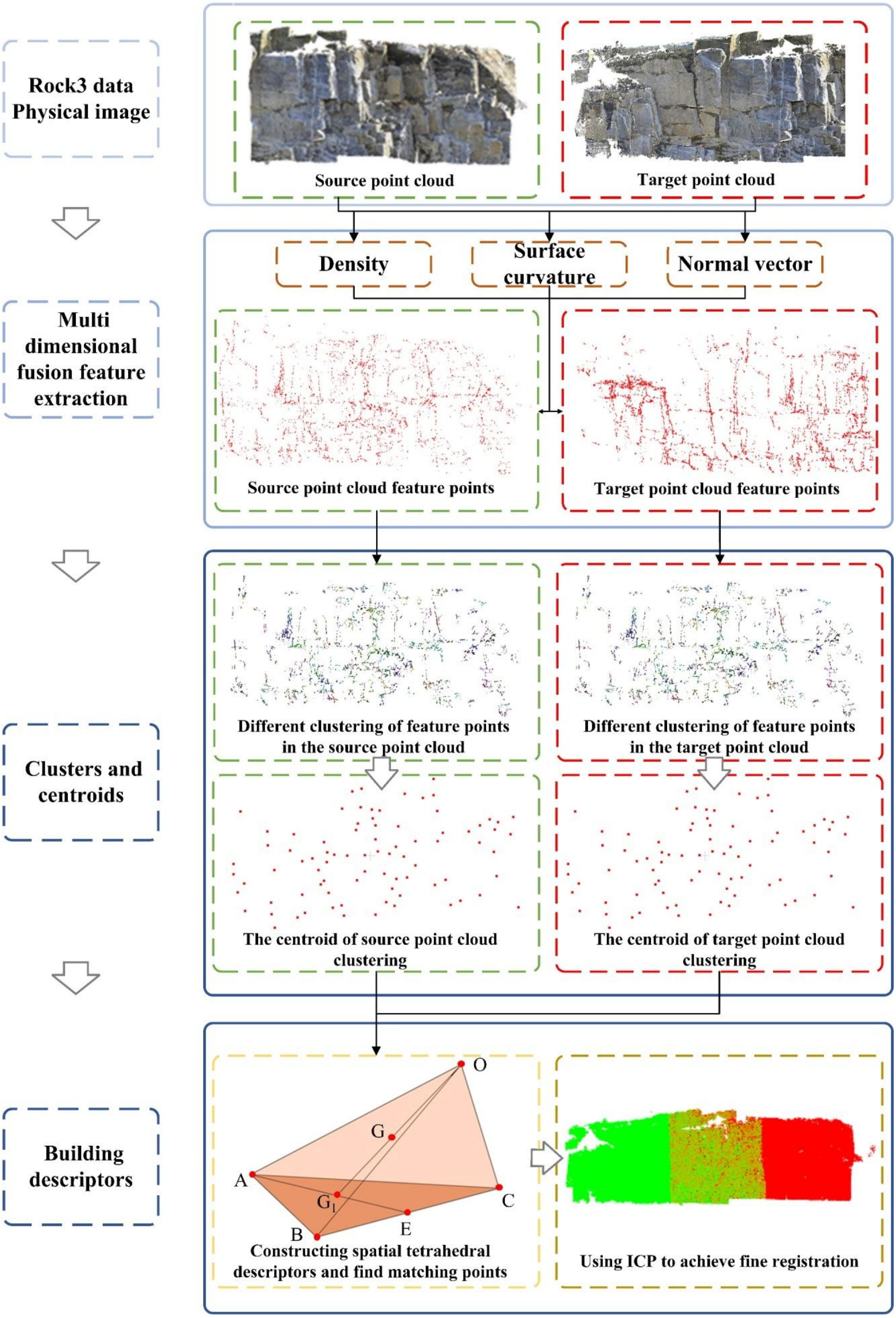

Figure 1. Registration Method Framework Preview

2.1 Rock Surface Feature Point Extraction

In this paper, we propose a multi-dimensional fusion feature point extraction method by combining the surface curvature, normal vector, and density features of point clouds.

1) Surface Curvature Variation

In point cloud data models, curvature information is widely used in data segmentation and simplification processing. The curvature of sharp features in point cloud data is relatively large. We use the method proposed by Jia et al. (2019) to perform weighted covariance analysis (PCA) on k neighboring points of a data point, estimating the curvature (surface variation factor) of the data point. Calculate its three eigenvalues λ_1, λ_2 and λ_3 using a weighted covariance matrix. If $\lambda_1 < \lambda_2 < \lambda_3$, then the change factor of the surface within the neighborhood of point p_i is:

$$\sigma_i = \frac{\lambda_1}{\lambda_1 + \lambda_2 + \lambda_3} \tag{1}$$

2) Normal Changes On The Surface

The normal vector can reflect the condition of the rock mass structural surfaces to a certain extent. Small changes in the normal vector indicate a flat rock surface, while larger changes suggest significant structural variations on the rock surface. Therefore, the degree of normal vector transformation can be used as a discriminant indicator for whether a point cloud is a feature point. The article adopts the normal vector variation rate calculation method proposed by Sanchez et al. (2020). The formula is as follows:

$$\mathrm{t}_i = \frac{1}{k}\sum_{j=1}^{k} n_i \cdot n_j \tag{2}$$

Where n_i represents the normal vector of *pi*, n_j represents the normal vector of the neighborhood points of p_i, and k is the number of neighborhood points.

3) Point Cloud Density Variation

Due to the variations in the angle and distance of point cloud acquisition, as well as the protruding structural planes on the rock surface, the density distribution of the rock mass point cloud is not uniform. The variation in density significantly affects the extraction of feature points.

Generally speaking, when data points are densely distributed, the average distance between their nearest neighbors is small, indicating that these points are located in the feature area; When the distribution of data points is sparse, the average distance between their nearest neighbors is large, indicating that these points are located in a smooth region (Wang et al., 2011).

We use the reciprocal of the average distance between point cloud data as the basis for calculating point cloud density, and represents the density of point P_i as:

$$\delta_i = \frac{1}{\frac{1}{k}\sum_{j=1}^{k}\left|d_{ij}\right|} \tag{3}$$

Integrate the obtained point cloud normal vector eigenvalues t_i, surface variation factor σ_i, and point cloud density δ_i as dimensionless parameter values, and define the feature parameters MFF of the data point p_i as follows:

$$MFF(p_i) = \frac{\frac{\delta_i - \delta_{\min}}{\delta_{\max} - \delta_{\min}} + \sigma_i}{t_i} \tag{4}$$

where $\delta_{\min}, \delta_{\max}$ are the minimum and maximum values of curvature in the data.

Points with M values greater than the given threshold are considered feature points of the rock mass, and they are used for clustering to locate the centroid points. The MeanShift clustering algorithm is used in this paper. The size of clusters is crucial for the quality of clustering and the accuracy of results. Large clusters may cover different geometric features, resulting in reduced accuracy of clustering results as they mix different surfaces and structures. Conversely, clustering that is small may not accurately reflect the actual structural features. Wang et al. (2019) have conducted relevant experiments in their article, which we will not elaborate on further.

The clustering process further reduces computational complexity. After obtaining the centroids of the effective clusters, we will directly use them to generate descriptors, treating these centroids as new feature points that are more representative.

2.2 Feature Description and Alignment of Corresponding Points

After obtaining the centroid, we need to find the intrinsic relationship between the source point cloud and the target point cloud. This article proposes a method of constructing descriptors by searching for tetrahedrons composed of centroids and domain feature points.

For a given point p_1, we search for the three nearest points of point p_1 through KD-tree. While ensuring that they are not coplanar, these four points will form a tetrahedron. As shown in Figure 2 (b), G is the center of gravity of the tetrahedron, G_1 is the center of gravity of the base triangle, and $OG = \frac{3}{4} OG_1$. We calculate the distance from each vertex to the centroid of the tetrahedron separately. If $p_i (i = 2,3,4)$ is the i-th nearest neighbor of p_i, then descriptor D is defined as:

$$D = (d_1, d_2, d_3, d_4) \quad (5)$$

where $d_i (i = 1,2,3,4)$ represents the distance from p_i to the center of gravity G, and the order of elements in D should correspond to the point sequence (p_1, p_2, p_3, p_4). L_{max}, L_{min} represent the maximum and minimum distances among the preceding four distances, respectively. α is the sum normal vector of the four points as angle constraints.

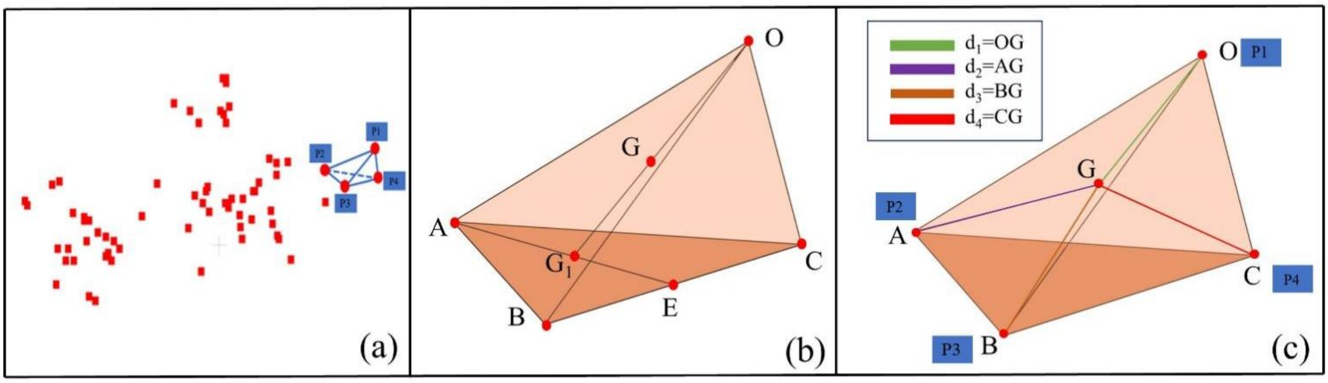

Figure 2. Construction method of descriptors. (a) Selected p_1 and the three nearest non coplanar neighbors. (b) Construct a spatial tetrahedron, where G is the center of gravity of the tetrahedron and G_1 is the center of gravity of the base triangle ABC. (c) Calculate the similarity between descriptors by calculating the distance between p_1, p_2, p_3, p_4 and the center of gravity G.

When the differences in L_{max}, L_{min}, and α between two feature points from the target point cloud and the source point cloud are each less than specific thresholds, the similarity between these two feature points is determined by calculating the Mahalanobis distance using the values of d1 ,d2.,d3,d4. The formula for similarity is as follows:

$$E(D_i, D_j^*) = \sqrt{(D_i, D_j^*)^T \sum\nolimits^{-1} (D_i, D_j^*)} \quad (6)$$

Where D_i and D_j^* respectively originate from the source point cloud and the target point cloud, $\sum$ is the covariance matrix constructed from D_i and D_j^*. The smaller E is, the higher the similarity between the two tetrahedrons, and the greater the probability that the described feature points are corresponding points. For a feature point i in the source point cloud, calculate $E(D_i, D_j^*)$ where j ranges from 1 to n (n being the number of feature points in the target point cloud). The point j with the smallest E value is determined to be the corresponding point for point i.

To improve the registration accuracy, we select the combination of three corresponding points with the highest similarity for registration. Subsequently, we randomly select several other combinations of corresponding points for registration, evaluate the registration accuracy of these combinations, and then use the optimal one in conjunction with the ICP algorithm to complete the final registration.

3. Experimental Results and Discussion

3.1 Datasets

The method proposed in this article is used for registration experiments on both public datasets and real scene datasets. The public dataset comes from the Rock bench database (Lato et al., 2013) and the WHU-TLS dataset (Dong et al., 2020) Rock1 in the public dataset is a single point cloud, and the target point cloud is obtained through rigid body transformation and truncation, Rock2 was captured by two different stations, both of which were from the Rock bench database. Rock3 comes from the WHU-TLS dataset. The real scene dataset was obtained from a dam in Jiangxi, China, scanned at different stations in different periods. A rock mass on the left side below the dam area was selected as the experimental data. The basic data information is shown in Table 1, Figure 3 and Figure 4.

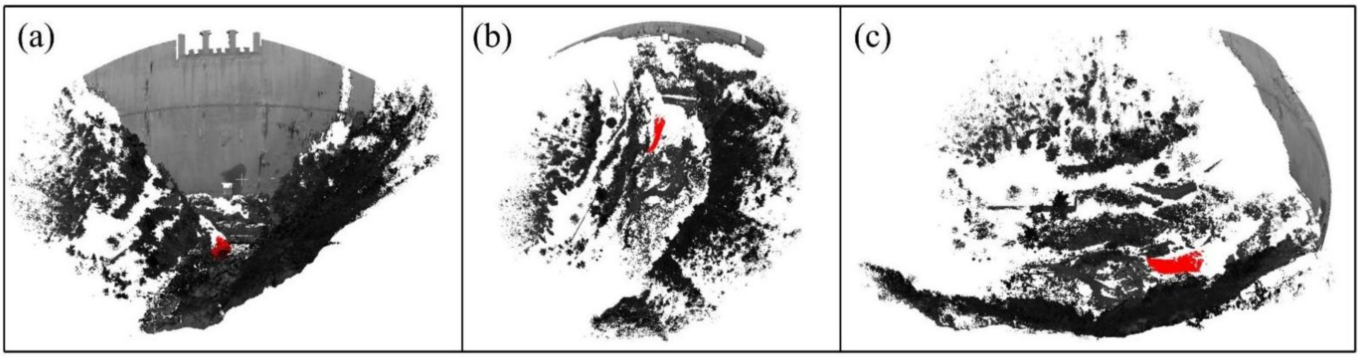

Figure 3. Visualization results from different perspectives in the dam area. (a) Main view. (b) vertical view. (c) Side view. The selected rock mass in the experiment is located in the lower left corner of the dam area，marked in red.

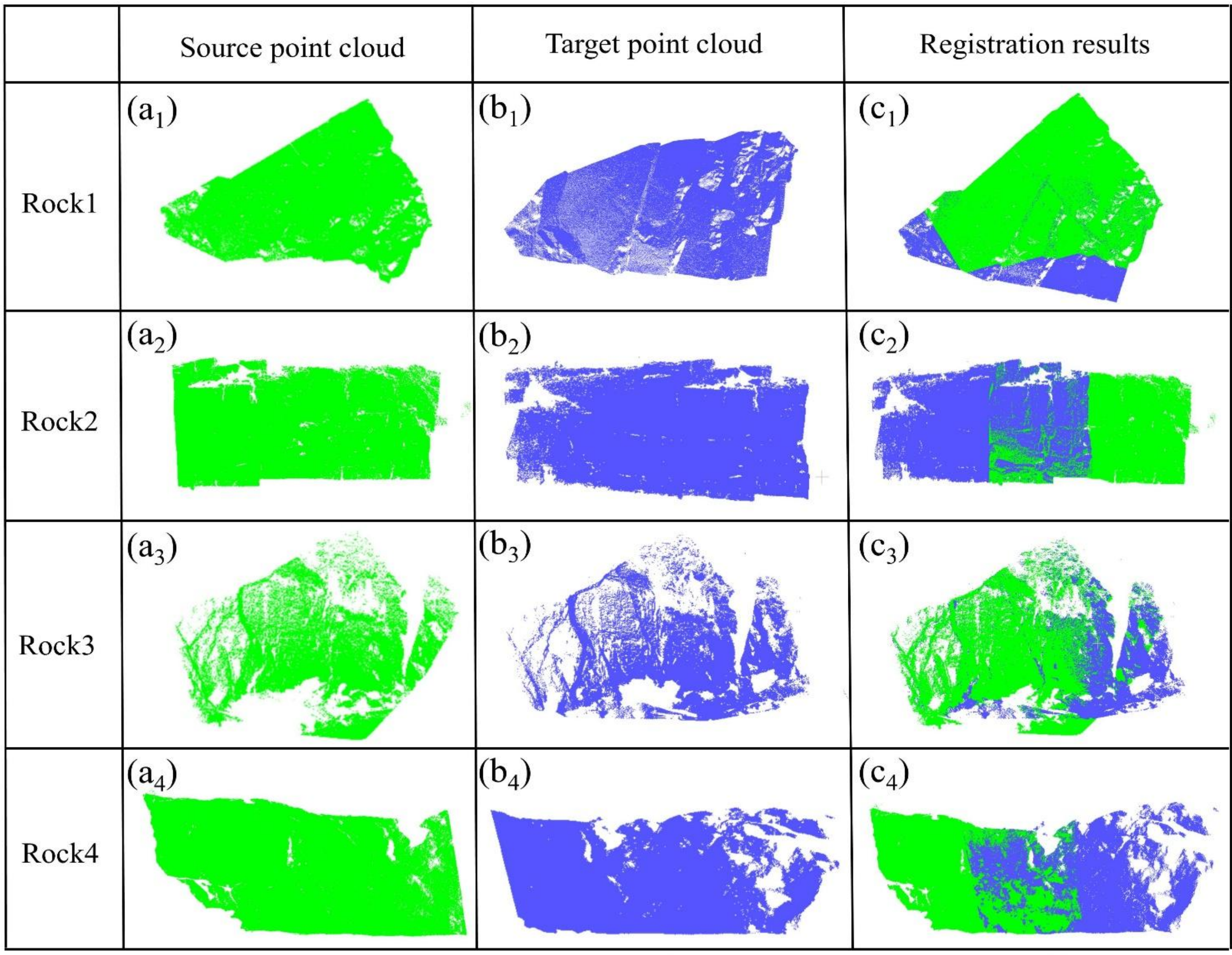

Figure 4. There are four different rock mass point clouds, (a_1)-(a_4) Source point cloud of rock1-rock4 rock mass. (b_1)-(b_4) Target point cloud of rock1-rock4 rock mass. (c_1)-(c_4) Registration results of rock1-rock4 rock masses obtained using the method described in this article.

Table 1. The number and overlap of point cloud data of different categories

parameter	Rock1		Rock2		Rock3		Rock4	
	Source point cloud	Target point cloud	Source point cloud	Target point cloud	Source point cloud	Target point cloud	Source point cloud	Target point cloud
points	887028	588917	1517037	1638869	2653426	3381901	1009442	993257
Overlap degree	≈55%		≈40%		≈75%		≈45%	

3.2 Analysis of Feature Extraction Results

In this paper, we extract feature points from Rock2 using methods based on Gaussian curvature, surface variance (Shi et al., 2018), normal vectors (Tao et al., 2016), SVF (Wang et al., 2021), and our proposed feature point extraction approach, respectively. Subsequently, these extracted feature points are utilized in the registration processes. The performance of these methods is compared and evaluated using the RMSE metric. To facilitate a fair comparison among the methods, the data processing scale is standardized with a neighborhood radius of 0.1 meters and a count of 10 neighboring points.

Figure 5 displays the rock mass feature points extracted by the aforementioned methods. Table 2 shows the number of feature points extracted by each method and the final calculated *RMSE* value. The normal vector method and the SVF extract a relatively large number of feature points. However, the feature points extracted by the normal vector method are inaccurate (Figure 5(c), (d)), resulting in the worst registration performance. The SVF method captures the structural feature points of the rock mass but also generates many redundant points (Figure 5(i), (j)). The surface curvature method extracts the least number of feature points, omitting many significant ones (Figure 5(e), (f)), which leads to low registration accuracy. The Gaussian curvature method yields a comparable number of feature points to our method, with the majority of these points being concentrated on the protruding structural characteristics of the rock mass. However, within the blue dashed-line box area, our method captures local fine features better (Figure 5(g), (h), (k), (l)), achieving higher registration accuracy.

The distribution accuracy of the feature points on the Figure 5 demonstrates a fundamental consistency with the registration precision outlined in the Table2. The final accuracy of the algorithm proposed in this paper is improved by 96.06%, 94.3%, 65.6%, and 77.8% over the previous four algorithms in that order. Therefore, accurately extracting feature points from point clouds is highly beneficial for the subsequent registration process.

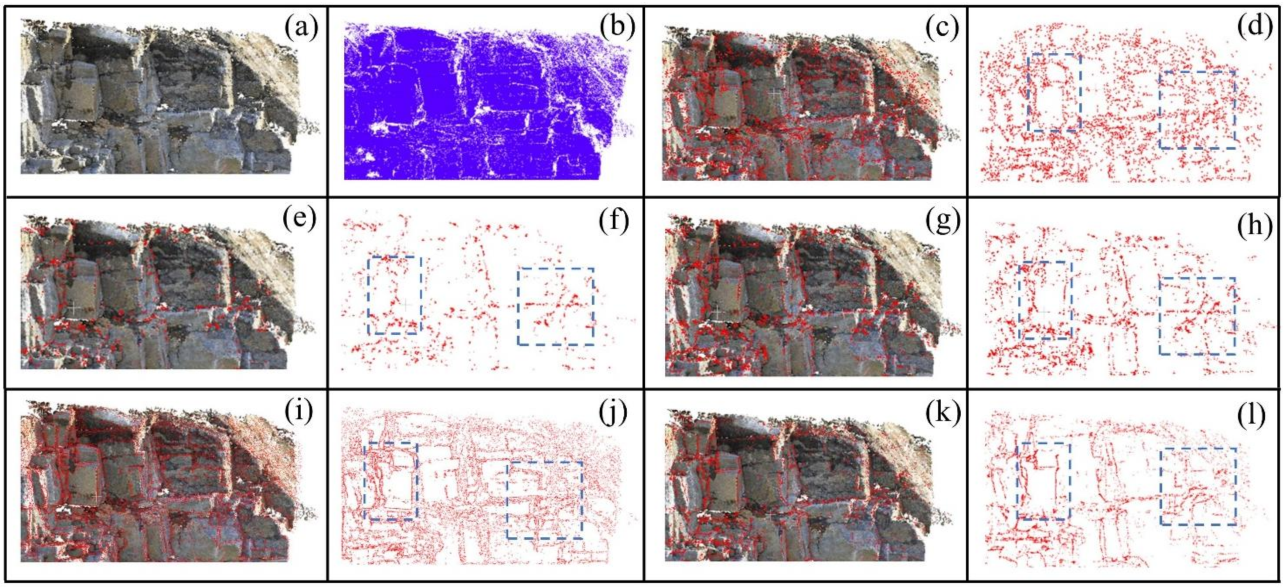

Figure 5. Detail maps of feature extraction results from various methods. (a) - (b) The entity map

and point cloud map of Rock2 data. (c) - (d) Schematic diagram of feature point extraction based on normal vectors. (e) - (f) Schematic diagram of feature points extracted based on curvature. (g) - (h) Schematic diagram of feature point extraction based on Gaussian curvature. (i) - (j) Schematic diagram of feature extraction using SVF algorithm. (k) - (l) Schematic diagram of the feature point extraction method proposed in this article. The figure outlines two parts of the rock mass structure that are more prominent.

Table 2. The number of feature points extracted and registration accuracy of each method

Methods	Number of feature points	RMSE/m
normal vectors	36285	0.05459
Surface curvature	11957	0.03774
Gaussian curvature	27994	0.00625
SVF	46741	0.00967
Ours	25465	0.00215

3.3 Analysis of Registration Results

1）Robustness Analysis

To verify the robustness of our registration method to the degree of overlap and initial position of point clouds, we conducted the following experiments.

Figure 6 shows the results of registration experiments conducted on the target point cloud of Rock1 after cutting it to different proportions, and then aligning it with the source point cloud. Table 3 demonstrates that our method maintains relatively stable registration accuracy across different degrees of overlap.

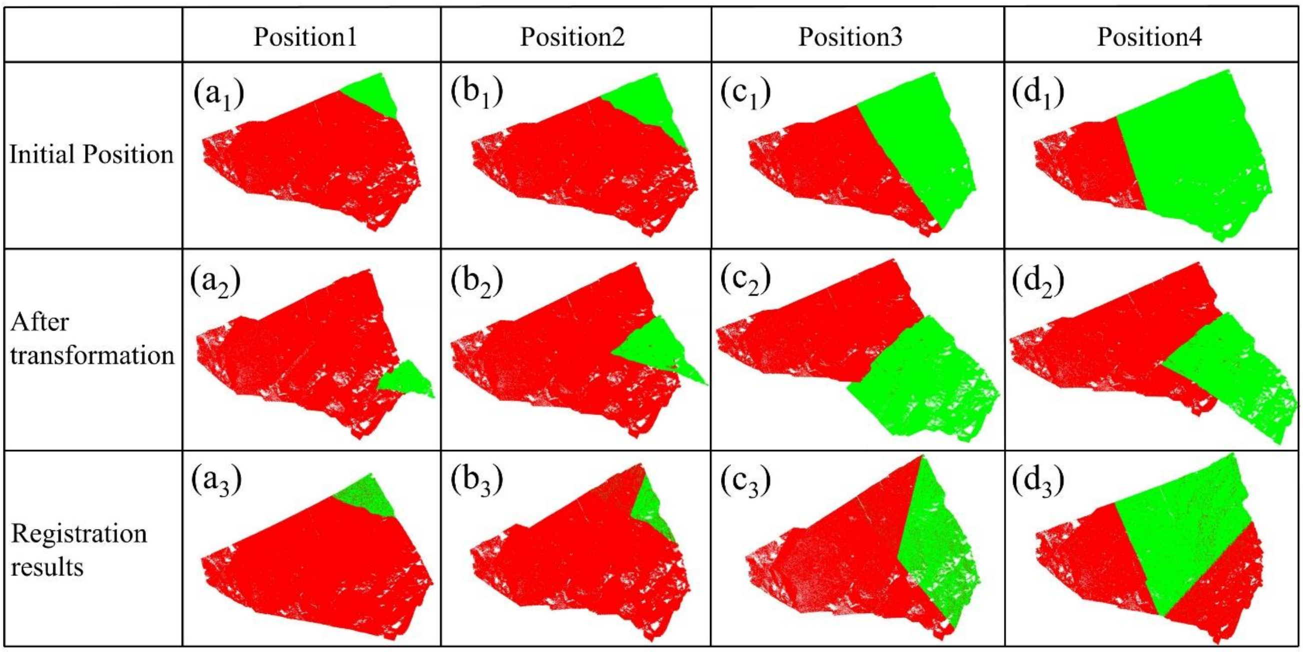

Figure 6. Experimental results for different degrees of overlap, the first row shows the original data in red, the segmented data in green, the second row shows the initial position of the data under the randomly assigned segmentation, and the third row shows the registration results. (a_1)-(a_3) Overlap degree of 20%. (b_1)-(b_3) Overlap degree of 30%. (c_1)-(c_3) Overlap degree of 55%. (d_1)-(d_3) Overlap degree of 70%.

Certain classic registration algorithms, such as ICP, exhibit high sensitivity to the initial position. Therefore, we applied various rigid transformations to the Rock1 data, placing it at distinct initial positions for the registration experiments. This approach aimed to verify the robustness of the algorithm proposed in this paper concerning the initial position. The Rock1 point clouds situated at these different locations are illustrated in Figure 7 (a)-(c), while Figure 7 (d) showcases the final registration outcomes. The RMSE values listed in Table 3 demonstrate that the method presented in this paper exhibits robustness to the initial position of the point cloud. This robustness stems from the fact that our method primarily relies on the extracted feature points to accomplish the registration, and variations in the initial position do not significantly impact the extraction of these feature points.

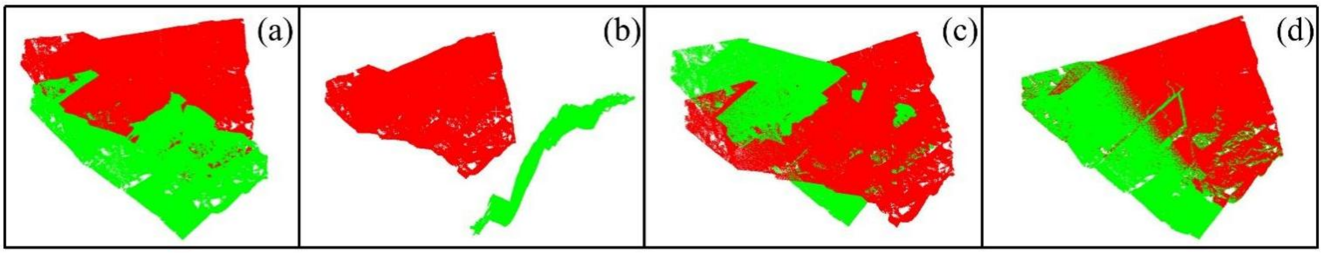

Figure 7. Registration experiments with different initial positions for Rock1. (a)-(c) show three different initial positions of Rock1 data, with the original data in red and the transformed positions in green. (d) shows the registration results, only one set of results is shown since the final results are approximately the same.

Table 3. Experimentation of point cloud data with different densities, overlaps, and initial positions using the proposed approach

Varying overlap degrees		Varying initial positions	
overlap degrees	RMSE/m	positions	RMSE/m
20%	0.00585	positions1	0.00397
30%	0.00487	positions2	0.00324
50%	0.00394	positions3	0.00415
70%	0.00416	Original position	0.00353

2) Accuracy Analysis

To assess the accuracy of the coarse registration method and compare it with traditional research methods, we employed K4PCS (Theiler et al., 2014), GROR (Yan et al., 2023), and FPFHSAC (Holz et al., 2015) for dataset registration. For parameter settings: K4PCS and FPFHSAC used a normal vector estimation radius of 0.3m and a voxel grid filter size of 0.1m during downsampling. FPFHSAC's feature estimation neighborhood radius was set to 1.2m. The number of iterations was set to 10000. GROR's voxel grid filter size during downsampling was set to 0.2m. All these methods can be implemented in PCL.

As shown in Table 4, the rotation and translation errors of different algorithms on each dataset are presented. The K4PCS algorithm performs poorly, likely due to uneven point cloud density distribution, which hinders feature point extraction. Similarly, the FPFHSAC algorithm may also suffer from this issue as feature estimation is sensitive to density variations, leading to larger translation errors. This occurs because variations in point density can produce different feature histograms for the same local shape feature in PFPH space, causing feature point matching errors. Both GORO and our proposed method achieved favorable results.

Our method emphasizes the importance of extracting complete and similar feature points, which is more adept at handling rock mass data with sharp structures. This is also the reason for the slightly lower registration results on the WHU-TLS dataset. Despite this, our coarse registration algorithm's results are satisfactory. Translation errors are greater than rotation errors due to inconsistency in feature points post-clustering, causing centroid deviations. For intuitive accuracy assessment, Figure 8 shows average error results.

Table 4. Quantitative evaluation of coarse registration accuracy

Data	Methods	Rotation error (deg)			Translation error (m)		
		X-axis rotation error	Y-axis rotation error	Z-axis rotation error	X-axis rotation error	Y-axis rotation error	Z-axis rotation error
Rock1	K4PCS	0.221	0.365	-0.654	-2.215	1.121	1.116
	FPFHSAC	0.965	0.548	0.152	1.212	-2.589	2.251
	GROR	0.654	-0.545	-0.215	-0.354	1.584	0.599
	OURS	0.254	0.321	-0.123	0.397	-0.991	0.155
Rock2	K4PCS	-0.252	0.219	-0.545	-1.835	3.837	0.744
	FPFHSAC	-0.104	0.152	-0.839	1.492	-0.926	1.716
	GROR	-0.318	-0.113	0.245	1.418	-0.256	-0.224
	OURS	0.318	0.362	0.093	-0.198	-0.468	-0.121
Rock3	K4PCS	0.225	-0.156	-0.451	2.615	0.655	1.165
	FPFHSAC	0.308	0.193	-0.280	5.715	-2.310	-0.352
	GROR	0.497	0.460	0.152	0.800	-0.179	0.571
	OURS	-0.234	-0.358	-0.116	0.631	0.217	0.132
Rock4	K4PCS	0.226	0.411	0.812	0.945	-2.541	1.597
	FPFHSAC	0.582	0.942	0.4621	0.335	1.215	-1.358
	GROR	0.138	0.540	-0.1658	0.396	0.323	-0.889
	OURS	0.100	0.412	-0.1560	0.699	-0.116	0.153

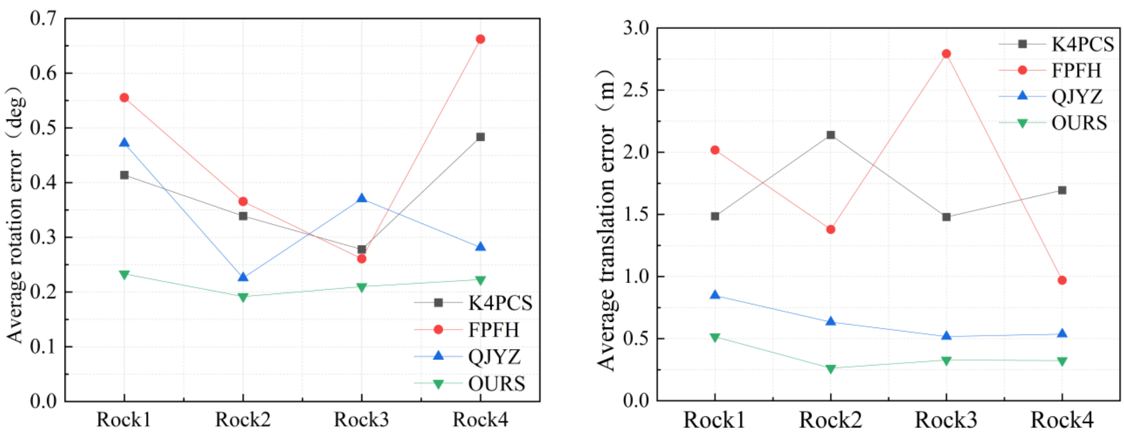

Figure 8. Comparison between average rotation error (a) and average translation error (b)

We used ICP algorithm（Besl et al., 1992）, LM-ICP algorithm（Fitzgibbon, 2003）, and 3D normal distribution 3D-NDT algorithm（Magnusson et al., 2007）for registration, and calculated the root mean square error of each method for performance comparison. The RMSE of the calculated results for each method is shown in the Table 5. Figure 9 shows the registration results of each dataset using different methods. We can see from the figure that most of the registration results are good visually. However, from the second row of the figure, we can see that the ICP algorithm is greatly limited by the initial position of the point cloud, and it falls into a local optimal solution when calculating Rock1 and Rock3 data. With good initial positions, the ICP algorithm can achieve satisfactory results. Therefore, the ICP algorithm cannot be directly used for rock mass point cloud registration. After obtaining a more accurate initial position through the coarse registration process, the method proposed in this paper greatly improves the accuracy of the registration results.

The LM-ICP algorithm introduces the chamfer distance transformation algorithm to replace the general KD tree search for nearest neighbors, improving the robustness to the initial position of the point cloud. Each rock mass point cloud data can calculate the final transformation matrix, and the accuracy is higher than the ICP algorithm, but not as high as the algorithm proposed in this paper. The NDT algorithm has a good registration effect on Rock1 point clouds that have undergone rigid body transformation, but its effect on partially overlapping Rock2 and Rock4 point clouds is average, and like the ICP algorithm, it cannot register Rock3 point clouds. Figure 9 and Table 5 fully demonstrate that the method proposed in this paper can be robust and accurate for the registration of rock mass point clouds.

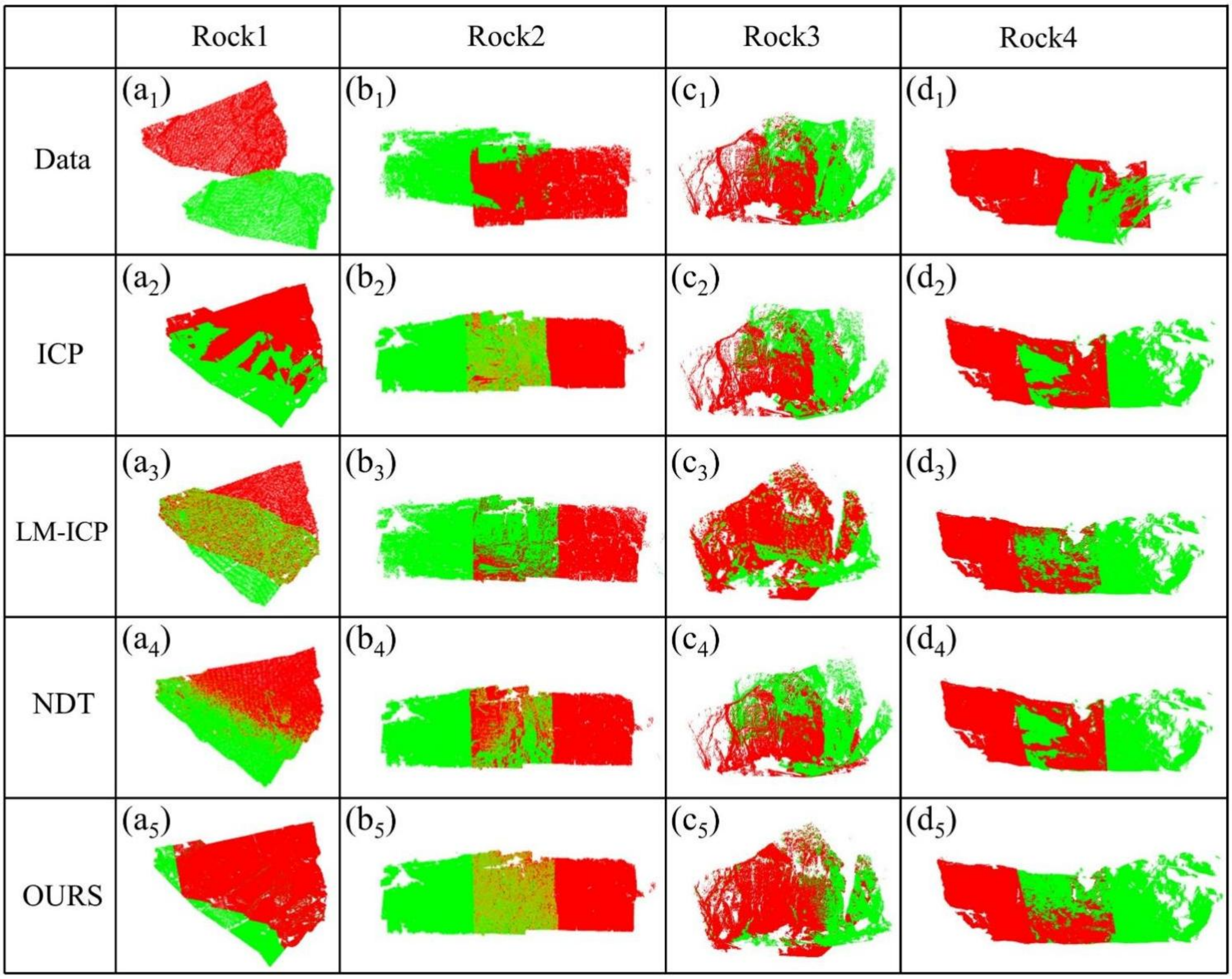

Figure 9. Comparison of registration results for different rock mass data methods. Red represents the source point cloud, and green represents the target point cloud. (a) Rock1 data. (b) Rock2 data. (c) Rock3 data. (d) Rock4 data.

Table 5. Quantitative evaluation of fine registration accuracy

Methods	RMSE/m			
	Rock1	Rock2	Rock3	Rock4
ICP	0.17521	0.00775	0.29618	0.08194
LM-ICP	0.04215	0.00351	0.06078	0.06154
DNT	0.00315	0.05575	0.24522	0.03948
OURS	0.00414	0.00215	0.05188	0.01334

4. Discussion

In this paper, we mainly study the problem of rock body point cloud registration and conduct experiments on public datasets and real scene datasets, from the initial feature point extraction to the final registration process, we propose a series of new ideas.

1) Our method is capable of extracting the protrusion features on the surface of rock masses, and is not limited to rock masses with distinct layering structures. Compared to registration methods based on line and surface features, it is applicable to a wider range of rock types. Three-dimensional laser scanning technology is the primary technique for collecting point clouds of large rock masses. However, variations in measurement distance and angle lead to uneven distribution of point cloud density, which in turn affects the effectiveness of feature extraction and registration. By incorporating density information during feature extraction, our method can appropriately improve the registration accuracy.

2) The spatial tetrahedron descriptor constructed in this paper has advantages in terms of ensuring the uniqueness of corresponding points. For rock masses with irregular structural distributions and lacking contextual information, it can better describe stable structures with rotation invariance from a global perspective, resulting in higher registration accuracy.

3) Our method, like current traditional methods, relies on the selection of certain parameter thresholds. These include: cluster radius r, distance threshold and angle threshold when matching descriptors。These parameters need to be set based on human experience, but they are basically related to the point cloud density. Furthermore, the centroid coordinates after clustering cannot accurately replace the positions of the original rock mass features, so our method can only serve as a coarse registration and needs to be combined with the ICP algorithm to achieve precise registration.

5. Conclusion

This article proposes a method for rock mass point cloud registration, which achieves rock mass alignment through feature point extraction and spatial description. The extraction of feature points integrates information on point cloud normal, curvature, and density, resulting in better performance for registering rock mass data with uneven density, particularly for large-scale rock masses captured by 3D laser scanners. By constructing spatial tetrahedral descriptors, the method can globally capture the spatial relationships of feature points, enabling more accurate identification of corresponding points between two datasets and achieving registration. When combined with the ICP algorithm, this method enables high-precision registration of rock mass point clouds, providing point cloud processing solutions for research on rock mass spatial shapes, surface structures, deformation detection, and other related studies.

Acknowledgements

This research is funded by Jiangxi Provincial Natural Science Foundation.(20232BAB204091), Thank you to Wu Xiang, Wang Yunbiao, and Wang Fengyan for generously providing repository data.

Reference

1. Besl P J, McKay N D, 1992. A method for registration of 3-D shapes[J]. IEEE Transactions on Pattern Analysis and Machine Intelligence, 14(2): 239-256.
2. Dong Z, Liang F, Yang B, et al, 2020. Registration of large-scale terrestrial laser scanner point clouds: A review and benchmark [J]. ISPRS Journal of Photogrammetry and Remote Sensing, 163: 327-342.
3. Fitzgibbon A W, 2003. Robust registration of 2D and 3D point sets[J]. Image and Vision Computing, 21(13-14): 1145-1153.
4. Frome A, Huber D, Kolluri R, et al. Recognizing Objects in Range Data Using Regional Point Descriptors[J].
5. Holz D, Ichim A E, Tombari F, et al., 2015. Registration with the Point Cloud Library: A Modular Framework for Aligning in 3-D[J]. IEEE Robotics & Automation Magazine, 22(4): 110-124.
6. Hu L, Xiao J, Wang Y, 2020. An automatic 3D registration method for rock mass point clouds based on plane detection and polygon matching [J]. The Visual Computer: International Journal of Computer Graphics, 36(4).
7. Huang F, Teng Z, Yao C, et al., 2024. Uncertainties of landslide susceptibility prediction: Influences of random errors in landslide conditioning factors and errors reduction by low pass filter method[J]. Journal of Rock Mechanics and Geotechnical Engineering, 16(1): 213-230.
8. Jia C C, Wang C J, Yang T, et al., 2019. A 3D Point Cloud Filtering Algorithm based on Surface Variation Factor Classification[J]. Procedia Computer Science, 154: 54-61.

9. Lato M, Kemeny J, Harrap R M, et al., 2013. Rock bench: Establishing a common repository and standards for assessing rockmass characteristics using LiDAR and photogrammetry[J]. Computers & Geosciences, 50: 106-114.
10. Liu L, Xiao J, Wang Yunbiao, et al., 2022. A Novel Rock-Mass Point Cloud Registration Method Based on Feature Line Extraction and Feature Point Matching[J]. IEEE Transactions on Geoscience and Remote Sensing, 60: 1-17.
11. Magnusson M, Lilienthal A, Duckett T, 2007. Scan registration for autonomous mining vehicles using 3D-NDT[J]. Journal of Field Robotics, 24(10): 803-827.
12. Rusu R B, Blodow N, Beetz M, 2009. Fast Point Feature Histograms (FPFH) for 3D registration[C]//2009 IEEE International Conference on Robotics and Automation. Kobe: IEEE: 3212-3217.
13. Sanchez J, Denis F, Coeurjolly D, et al., 2020. Robust normal vector estimation in 3D point clouds through iterative principal component analysis[J]. ISPRS Journal of Photogrammetry and Remote Sensing, 163: 18-35.
14. Shi X, Ren J, Ren XK, 2018. Drift registration method based on curvature features, Laser & Optoelectronics Progress[J], 55(8): 248-254
15. Tao HJ, Da FP, 2013. A point cloud automatic registration method based on normal vectors [J]. Chinese Journal of Lasers, 40(8): 184-189.
16. Theiler P W, Wegner J D, Schindler K, 2014.Keypoint-based 4-Points Congruent Sets – Automated marker-less registration of laser scans[J]. ISPRS Journal of Photogrammetry and Remote Sensing, 96: 149-163.
17. Tombari F, Salti S, Stefano L D. Unique Signatures of Histograms for Local Surface Description[J].
18. Wang F, Xiao J, Wang Y, 2019. Efficient Rock-Mass Point Cloud Registration Using n-Point Complete Graphs[J]. IEEE TRANSA CTIONS ON GEOSCIENCE AND REMOTE SENSING, 57(11).
19. Wang Yunbiao, Xiao J, Liu L, et al., 2021. Efficient Rock Mass Point Cloud Registration Based on Local Invariants[J]. Remote Sensing, 13(8): 1540.
20. Wang LH, Yuan BZ, 2011. Feature point detection of 3D scattered point cloud model[J]. Signal Processing, 27(6): 932-938.
21. Warchol D, 2018. HAND POSTURE RECOGNITION USING MODIFIED ENSEMBLE OF SHAPE FUNCTIONS AND GLOBAL RADIUS-BASED SURFACE DESCRIPTOR [J]. Computer Science, 19(2): 115.
22. Yan L, Wei P, Xie H, et al., 2023. A New Outlier Removal Strategy Based on Reliability of Correspondence Graph for Fast Point Cloud Registration[J]. IEEE Transactions on Pattern Analysis and Machine Intelligence, 45(7): 79 86-8002.